

# Radiative transitions of the helium atom in highly magnetized neutron star atmospheres

Z. Medin,<sup>1</sup>\* D. Lai<sup>1</sup> and A. Y. Potekhin<sup>1,2</sup>

<sup>1</sup>Centre for Radiophysics and Space Research, Department of Astronomy, Cornell University, Ithaca, NY 14853, USA

<sup>2</sup>Ioffe Physico-Technical Institute, Politekhnicheskaya 26, 194021 Saint-Petersburg, Russia

Accepted 2007 September 26. Received 2007 May 21; in original form 2007 April 12

## ABSTRACT

Recent observations of thermally emitting isolated neutron stars revealed spectral features that could be interpreted as radiative transitions of He in a magnetized neutron star atmosphere. We present Hartree–Fock calculations of the polarization-dependent photoionization cross-sections of the He atom in strong magnetic fields ranging from  $10^{12}$  to  $10^{14}$  G. Convenient fitting formulae for the cross-sections are given along with the related oscillator strengths for various bound–bound transitions. The effects of finite nucleus mass on the radiative absorption cross-sections are examined using perturbation theory.

**Key words:** atomic processes – magnetic fields – stars: atmospheres – stars: neutron.

## 1 INTRODUCTION

An important advance in neutron star (NS) astrophysics in the last few years has been the detection and detailed studies of surface emission from a large number of isolated NSs, including radio pulsars, magnetars and radio-quiet NSs (e.g. Harding & Lai 2006; Kaspi, Roberts & Harding 2006). This was made possible by X-ray telescopes such as *Chandra* and *XMM–Newton*. Such studies can potentially provide invaluable information on the physical properties and evolution of NSs (e.g. equation of state at super-nuclear densities, cooling history, surface magnetic field and composition). Of great interest are the radio-quiet, thermally emitting NSs (e.g. Haberl 2006): they share the common property that their spectra appear to be entirely thermal, indicating that the emission arises directly from the NS surfaces, uncontaminated by magnetospheric emission. The true nature of these sources, however, is unclear at present: they could be young cooling NSs, or NSs kept hot by accretion from the interstellar medium, or magnetar descendants. While some of these NSs (e.g. RX J1856.5–3754) have featureless X-ray spectrum remarkably well described by blackbody (e.g. Burwitz et al. 2003) or by emission from a condensed surface covered by a thin atmosphere (Ho et al. 2007), single- or multiple-absorption features at  $E \simeq 0.2$ –1 keV have been detected from several sources (see van Kerkwijk & Kaplan 2007): e.g. 1E 1207.4–5209 (0.7 and 1.4 keV, possibly also 2.1, 2.8 keV; Sanwal et al. 2002; De Luca et al. 2004; Mori, Chonko & Hailey 2005), RX J1308.6+2127 (0.2–0.3 keV; Haberl et al. 2003), RX J1605.3+3249 (0.45 keV; van Kerkwijk et al. 2004), RX J0720.4–3125 (0.27 keV; Haberl et al. 2006) and possibly RBS 1774 ( $\sim 0.7$  keV; Zane et al. 2005). The identifications of these features, however, remain uncertain, with suggestions ranging from proton cyclotron lines to atomic transitions of H, He or

mid-Z atoms in a strong magnetic field (see Sanwal et al. 2002; Ho & Lai 2004; Pavlov & Bezchastnov 2005; Mori & Ho 2007). Clearly, understanding these absorption lines is very important as it would lead to direct measurement of the NS surface magnetic fields and compositions, shedding light on the nature of these objects. Multiple lines also have the potential of constraining the mass–radius relation of NSs (through the measurement of gravitational redshift).

Since the thermal radiation from a NS is mediated by its atmosphere (if  $T$  is sufficiently high so that the surface does not condense into a solid; see e.g. van Adelsberg et al. 2005; Medin & Lai 2006, 2007), detailed modelling of radiative transfer in magnetized NS atmospheres is important. The atmosphere composition of the NS is unknown a priori. Because of the efficient gravitational separation of light and heavy elements, a pure H atmosphere is expected even if a small amount of fallback or accretion occurs after NS formation. A pure He atmosphere results if H is completely burnt out, and a heavy-element (e.g. Fe) atmosphere may be possible if no fallback/accretion occurs. The atmosphere composition may also be affected by (slow) diffusive nuclear burning in the outer NS envelope (Chang, Arras & Bildsten 2004), as well as by the bombardment on the surface by fast particles from NS magnetospheres (e.g. Beloborodov & Thompson 2007). Fully ionized atmosphere models in various magnetic field regimes have been extensively studied (e.g. Shibano et al. 1992; Ho & Lai 2001; Zane et al. 2001), including the effect of vacuum polarization (see Lai & Ho 2002, 2003; Ho & Lai 2003; van Adelsberg & Lai 2006). Because a strong magnetic field greatly increases the binding energies of atoms, molecules and other bound species (for a review, see Lai 2001), these bound states may have appreciable abundances in the NS atmosphere, as guessed by Cohen, Lodenquai & Ruderman (1970) and confirmed by calculations of Lai & Salpeter (1997) and Potekhin, Chabrier & Shibano (1999). Early considerations of partially ionized and strongly magnetized atmospheres (e.g. Rajagopal, Romani & Miller 1997) relied on oversimplified

\*E-mail: zach@astro.cornell.edu

treatments of atomic physics and plasma thermodynamics (ionization equilibrium, equation of state and non-ideal plasma effects). Recently, a thermodynamically consistent equation of state and opacities for magnetized ( $B = 10^{12}$ – $10^{15}$  G), partially ionized H plasma have been obtained (Potekhin & Chabrier 2003, 2004), and the effect of bound atoms on the dielectric tensor of the plasma has also been studied (Potekhin et al. 2004). These improvements have been incorporated into partially ionized, magnetic NS atmosphere models (Ho et al. 2003, 2007; Potekhin et al. 2004, 2006). Mid-Z element atmospheres for  $B \sim 10^{12}$ – $10^{13}$  G were recently studied by Mori & Ho (2007).

In this paper, we focus on He atoms and their radiative transitions in magnetic NS atmospheres. It is well known that for  $B \gg Z^2 B_0$ , where  $Z$  is the charge number of the nucleus and  $B_0 = e^3 m_e^2 / \hbar^3 c = 2.35 \times 10^9$  G, the binding energy of an atom is significantly increased over its zero-field value. In this *strong-field regime*, the electrons are confined to the ground Landau level, and one may apply the *adiabatic approximation*, in which electron motions along and across the field are assumed to be decoupled from each other (see Section 2.1). Using this approximation in combination with the Hartree–Fock method (‘1DHF approximation’), several groups calculated binding energies for the helium atom (Pröschel et al. 1982; Thurner et al. 1993) and also for some other atoms and molecules (Neuhauser, Langanke & Koonin 1986; Neuhauser, Koonin & Langanke 1987; Miller & Neuhauser 1991; Lai, Salpeter & Shapiro 1992). Mori & Hailey (2002) developed a ‘multiconfigurational perturbative hybrid Hartree–Fock’ approach, which is a perturbative improvement of the 1DHF method. Other methods of calculation include Thomas–Fermi-like models (e.g. Abrahams & Shapiro 1991), the density functional theory (e.g. Relovsky & Ruder 1996; Medin & Lai 2006), variational methods (e.g. Müller 1984; Vincke & Baye 1989; Jones, Ortiz & Ceperley 1999; Turbiner & Guevara 2006) and 2D Hartree–Fock mesh calculations (Ivanov 1994; Ivanov & Schmelcher 2000) which do not directly employ the adiabatic approximation.

In strong magnetic fields, the finite nuclear mass and centre-of-mass motion affect the atomic structure in a non-trivial way (e.g. Lai 2001; see Section 5). The stronger  $B$  is, the more important the effects of finite nuclear mass are. Apart from the H atom, these effects have been calculated only for the He atom which *rests as a whole*, but has a moving nucleus (Al-Hujaj & Schmelcher 2003a,b), and for the  $\text{He}^+$  ion (Bezchastnov, Pavlov & Ventura 1998; Pavlov & Bezchastnov 2005).

There were relatively few publications devoted to radiative transitions of non-hydrogenic atoms in strong magnetic fields. Several authors (Miller & Neuhauser 1991; Thurner et al. 1993; Jones et al. 1999; Mori & Hailey 2002; Al-Hujaj & Schmelcher 2003b) calculated oscillator strengths for bound–bound transitions; Miller & Neuhauser (1991) also presented a few integrated bound–free oscillator strengths. Rajagopal et al. (1997) calculated opacities of strongly magnetized iron, using photoionization cross-sections obtained by M. C. Miller (unpublished). To the best of our knowledge, there were no published calculations of polarization-dependent photoionization cross-sections for the He atom in the strong-field regime, as well as the calculations of the atomic motion effect on the photoabsorption coefficients for He in this regime. Moreover, the subtle effect of exchange interaction involving free electrons and the possible role of two-electron transitions (see Section 3.2) have not been discussed before.

In this paper, we perform detailed calculations of radiative transitions of the He atom using the 1DHF approximation. The total error introduced into our calculations by the use of these two

approximations, the Hartree–Fock method and the adiabatic approximation is of the order of 1 per cent or less, as can be seen by the following considerations: the Hartree–Fock method is approximate because electron correlations are neglected. Due to their mutual repulsion, any pair of electrons tends to be more distant from each other than the Hartree–Fock wavefunction would indicate. In zero-field, this correlation effect is especially pronounced for the spin-singlet states of electrons for which the spatial wavefunction is symmetrical. In strong magnetic fields ( $B \gg B_0$ ), the electron spins (in the ground state) are all aligned antiparallel to the magnetic field, and the multielectron spatial wavefunction is antisymmetric with respect to the interchange of two electrons. Thus, the error in the Hartree–Fock approach is expected to be less than the 1 per cent accuracy characteristic of zero-field Hartree–Fock calculations (Neuhauser et al. 1987; for  $B = 0$  see Scrinzi 1998; Schmelcher, Ivanov & Becken 1999). The adiabatic approximation is also very accurate at  $B \gg Z^2 B_0$ . Indeed, a comparison of the ground-state energy values calculated here to those of Ivanov (1994) (who did not use the adiabatic approximation) shows an agreement to within 1 per cent for  $B = 10^{12}$  G and to within 0.1 per cent for  $B = 10^{13}$  G.

This paper is organized as follows. Section 2 describes our calculations of the bound states and continuum states of the He atom, and Section 3 contains relevant equations for radiative transitions. We present our numerical results and fitting formulae in Section 4 and examine the effects of finite nucleus mass on the photoabsorption cross-sections in Section 5.

## 2 BOUND STATES AND SINGLY IONIZED STATES OF HELIUM ATOMS IN STRONG MAGNETIC FIELDS

### 2.1 Bound states of the helium atom

To define the notation, we briefly describe 1DHF calculations for He atoms in strong magnetic fields. Each electron in the atom is described by a one-electron wavefunction (orbital). If the magnetic field is sufficiently strong (e.g.  $B \gg 10^{10}$  G for He ground state), the motion of an electron perpendicular to the magnetic field lines is mainly governed by the Lorentz force, which is, on the average, stronger than the Coulomb force. In this case, the adiabatic approximation can be employed – i.e. the wavefunction can be separated into a transverse (perpendicular to the external magnetic field) component and a longitudinal (along the magnetic field) component:

$$\phi_{m\nu}(\mathbf{r}) = f_{m\nu}(z)W_m(\mathbf{r}_\perp). \quad (1)$$

Here,  $W_m$  is the ground-state Landau wavefunction (e.g. Landau & Lifshitz 1977) given by

$$W_m(\mathbf{r}_\perp) = \frac{1}{\rho_0 \sqrt{2\pi m!}} \left( \frac{\rho}{\sqrt{2}\rho_0} \right)^m \exp\left( \frac{-\rho^2}{4\rho_0^2} \right) e^{-im\varphi}, \quad (2)$$

where  $(\rho, \varphi)$  are the polar coordinates of  $\mathbf{r}_\perp$ ,  $\rho_0 = (\hbar c/eB)^{1/2}$  is the magnetic length and  $f_{m\nu}$  is the longitudinal wavefunction which can be calculated numerically. The quantum number  $m$  ( $\geq 0$  for the considered ground Landau state) specifies the *negative* of the  $z$ -projection of the electron orbital angular momentum. We restrict our consideration to electrons in the ground Landau level; for these electrons,  $m$  also specifies the (transverse) distance of the guiding centre of the electron from the ion,  $\rho_m = (2m + 1)^{1/2} \rho_0$ . The quantum number  $\nu$  specifies the number of nodes in the longitudinal wavefunction. The spins of the electrons are taken to be aligned antiparallel with the magnetic field, and so do not enter into any

of our equations. In addition, we assume that the ion is completely stationary (the ‘infinite ion mass’ approximation). In general, the latter assumption is not necessary for the applicability of the adiabatic approximation (see e.g. Potekhin 1994). The accuracy of the infinite ion mass approximation will be discussed in Section 5.

Note that we use non-relativistic quantum mechanics in our calculations, even when  $\hbar\omega_{Be} \gtrsim m_e c^2$  or  $B \gtrsim B_Q = B_0/\alpha^2 = 4.414 \times 10^{13}$  G. This is valid for two reasons: (i) the free-electron energy in relativistic theory is

$$E = \left[ c^2 p_z^2 + m_e^2 c^4 \left( 1 + 2n_L \frac{B}{B_Q} \right) \right]^{1/2}. \quad (3)$$

For electrons in the ground Landau level ( $n_L = 0$ ), equation (3) reduces to  $E \simeq m_e c^2 + p_z^2/(2m_e)$  for  $p_z c \ll m_e c^2$ ; the electron remains non-relativistic in the  $z$  direction as long as the electron energy is much less than  $m_e c^2$ ; (ii) it is well known (e.g. Sokolov & Ternov 1986) that equation (2) describes the transverse motion of an electron with  $n_L = 0$  at any field strength, and thus equation (2) is valid in the relativistic theory. Our calculations assume that the longitudinal motion of the electron is non-relativistic. This is valid for helium at all field strengths considered in this paper. Thus, relativistic corrections to our calculated electron wavefunctions, binding energies and transition cross-sections are all small. Our approximation is justified in part by Chen & Goldman (1992), who find that the relativistic corrections to the binding energy of the hydrogen atom are of the order of  $\Delta E/E \sim 10^{-5.5} - 10^{-4.5}$  for the range of field strengths we are considering in this work ( $B = 10^{12} - 10^{14}$  G).

A bound state of the He atom, in which one electron occupies the  $(m_1 \nu_1)$  orbital, and the other occupies the  $(m_2 \nu_2)$  orbital, is denoted by  $|m_1 \nu_1, m_2 \nu_2\rangle = |W_{m_1} f_{m_1 \nu_1}, W_{m_2} f_{m_2 \nu_2}\rangle$  (clearly,  $|m_1 \nu_1, m_2 \nu_2\rangle = |m_2 \nu_2, m_1 \nu_1\rangle$ ). The two-electron wavefunction is

$$\Psi_{m_1 \nu_1, m_2 \nu_2}(\mathbf{r}_1, \mathbf{r}_2) = \frac{1}{\sqrt{2}} \left[ W_{m_1}(\mathbf{r}_{1\perp}) f_{m_1 \nu_1}(z_1) \times W_{m_2}(\mathbf{r}_{2\perp}) f_{m_2 \nu_2}(z_2) - W_{m_2}(\mathbf{r}_{1\perp}) f_{m_2 \nu_2}(z_1) W_{m_1}(\mathbf{r}_{2\perp}) f_{m_1 \nu_1}(z_2) \right]. \quad (4)$$

The one-electron wavefunctions are found using Hartree–Fock theory, by varying the total energy with respect to the wavefunctions. The total energy is given by (see e.g. Neuhauser et al. 1987)

$$E = E_K + E_{eZ} + E_{\text{dir}} + E_{\text{exc}}, \quad (5)$$

where

$$E_K = \frac{\hbar^2}{2m_e} \sum_{mv} \int dz |f'_{mv}(z)|^2, \quad (6)$$

$$E_{eZ} = -Ze^2 \sum_{mv} \int dz |f_{mv}(z)|^2 V_m(z), \quad (7)$$

$$E_{\text{dir}} = \frac{e^2}{2} \sum_{mv, m'v'} \iint dz dz' |f_{mv}(z)|^2 |f_{m'v'}(z')|^2 \times D_{mm'}(z - z'), \quad (8)$$

$$E_{\text{exc}} = -\frac{e^2}{2} \sum_{mv, m'v'} \iint dz dz' f_{m'v'}^*(z) f_{mv}(z) \times f_{mv}^*(z') f_{m'v'}(z') E_{mm'}(z - z') \quad (9)$$

and

$$V_m(z) = \int d\mathbf{r}_\perp \frac{|W_m(\mathbf{r}_\perp)|^2}{r}, \quad (10)$$

$$D_{mm'}(z - z') = \iint d\mathbf{r}_\perp d\mathbf{r}'_\perp \frac{|W_m(\mathbf{r}_\perp)|^2 |W_{m'}(\mathbf{r}'_\perp)|^2}{|\mathbf{r}' - \mathbf{r}|}, \quad (11)$$

$$E_{mm'}(z - z') = \iint d\mathbf{r}_\perp d\mathbf{r}'_\perp \frac{1}{|\mathbf{r}' - \mathbf{r}|} \times W_{m'}^*(\mathbf{r}_\perp) W_m(\mathbf{r}_\perp) W_m^*(\mathbf{r}'_\perp) W_{m'}(\mathbf{r}'_\perp). \quad (12)$$

Variation of equation (5) with respect to  $f_{mv}(z)$  yields

$$\left[ -\frac{\hbar^2}{2m_e} \frac{d^2}{dz^2} - Ze^2 V_m(z) + e^2 \sum_{m'v'} \int dz' |f_{m'v'}(z')|^2 D_{mm'}(z - z') - \varepsilon_{mv} \right] f_{mv}(z) = e^2 \sum_{m'v'} \int dz' f_{m'v'}^*(z') f_{m'v'}(z') E_{mm'}(z - z') f_{m'v'}(z). \quad (13)$$

In these equations, asterisks denote complex conjugates, and  $f'_{mv}(z) \equiv df_{mv}/dz$ . The wavefunctions  $f_{mv}(z)$  must satisfy appropriate boundary conditions, i.e.  $f_{mv} \rightarrow 0$  as  $z \rightarrow \pm\infty$ , and must have the required symmetry [ $f_{mv}(z) = \pm f_{mv}(-z)$ ] and the required number of nodes ( $\nu$ ). The equations are solved iteratively until self-consistency is reached for each wavefunction  $f_{mv}$  and energy  $\varepsilon_{mv}$ . The total energy of the bound He state  $|m_1 \nu_1, m_2 \nu_2\rangle$  can then be found, using either equation (5) or

$$E = \sum_{mv} \varepsilon_{mv} - E_{\text{dir}} - E_{\text{exc}}. \quad (14)$$

## 2.2 Continuum states of the helium atom

The He state in which one electron occupies the bound  $(m_3 \nu_3)$  orbital, and other occupies the continuum state  $(m_4 k)$  is denoted by  $|m_3 \nu_3, m_4 k\rangle = |W_{m_3} f_{m_3 \nu_3}, W_{m_4} f_{m_4 k}\rangle$ . The corresponding two-electron wavefunction is

$$\Psi_{m_3 \nu_3, m_4 k}(\mathbf{r}_1, \mathbf{r}_2) = \frac{1}{\sqrt{2}} \left[ W_{m_3}(\mathbf{r}_{1\perp}) f_{m_3 \nu_3}(z_1) \times W_{m_4}(\mathbf{r}_{2\perp}) f_{m_4 k}(z_2) - W_{m_4}(\mathbf{r}_{1\perp}) f_{m_4 k}(z_1) W_{m_3}(\mathbf{r}_{2\perp}) f_{m_3 \nu_3}(z_2) \right]. \quad (15)$$

Here,  $f_{m_4 k}(z)$  is the longitudinal wavefunction of the continuum electron and  $k$  is the  $z$ -wavenumber of the electron at  $|z| \rightarrow \infty$  (far away from the He nucleus).

We can use Hartree–Fock theory to solve for the ionized He states as we did for the bound He states. Since the continuum electron wavefunction  $f_{m_4 k}(z)$  is non-localized in  $z$ , while the bound electron wavefunction  $f_{m_3 \nu_3}(z)$  is localized around  $z = 0$ , it is a good approximation to neglect the continuum electron’s influence on the bound electron. We therefore solve for the bound electron orbital using the equation

$$\left[ -\frac{\hbar^2}{2m_e} \frac{d^2}{dz^2} - Ze^2 V_{m_3}(z) \right] f_{m_3 \nu_3}(z) = \varepsilon_{m_3 \nu_3} f_{m_3 \nu_3}(z). \quad (16)$$

The continuum electron, however, is influenced by the bound electron, and its longitudinal wavefunction is determined from

$$\left[ -\frac{\hbar^2}{2m_e} \frac{d^2}{dz^2} - Ze^2 V_{m_4}(z) + e^2 \int dz' |f_{m_3 \nu_3}(z')|^2 D_{m_3 m_4}(z - z') - \varepsilon_f \right] f_{m_4 k}(z) = e^2 \int dz' f_{m_4 k}^*(z') f_{m_3 \nu_3}(z') E_{m_3 m_4}(z - z') f_{m_3 \nu_3}(z), \quad (17)$$

where  $\varepsilon_f = \varepsilon_{m_4k} = \hbar^2 k^2 / (2m_e)$ . Here, the bound electron orbital  $|m_3\nu_3\rangle$  satisfies the same boundary conditions as discussed in Section 2.1. The shape of the free electron wavefunction is determined by the energy of the incoming photon and the direction the electron is emitted from the ion. We will discuss this boundary condition in the next section. The total energy of the ionized He state  $|m_3\nu_3, m_4k\rangle$  is simply

$$E = \varepsilon_{m_3\nu_3} + \varepsilon_f. \quad (18)$$

Note that the correction terms  $E_{\text{dir}}$  and  $E_{\text{exc}}$  that appear in equation (14) do not also appear in equation (18). The direct and exchange energies depend on the local overlap of the electron wavefunctions, but the non-localized nature of the free electron ensures that these terms are zero for the continuum states.

### 3 RADIATIVE TRANSITIONS

We will be considering transitions of helium atoms from two initial states: the ground state,  $|00, 10\rangle$ , and the first excited state,  $|00, 20\rangle$ .

In the approximation of an infinitely massive, point-like nucleus, the Hamiltonian of the He atom in electromagnetic field is (see e.g. Landau & Lifshitz 1977)

$$H = \sum_{j=1,2} \frac{1}{2m_e} \left[ \mathbf{p}_j + \frac{e}{c} \mathbf{A}_{\text{tot}}(\mathbf{r}_j) \right]^2 - \sum_{j=1,2} \frac{2e^2}{r_j^2} + \frac{e^2}{|\mathbf{r}_1 - \mathbf{r}_2|}, \quad (19)$$

where  $\mathbf{p}_j = -i\hbar\nabla_j$  is the canonical momentum operator, acting on the  $j$ th electron,  $\mathbf{r}_j$  is the  $j$ th electron radius vector, measured from the nucleus, and  $\mathbf{A}_{\text{tot}}(\mathbf{r})$  is the vector potential of the field. In our case,  $\mathbf{A}_{\text{tot}}(\mathbf{r}) = \mathbf{A}_B(\mathbf{r}) + \mathbf{A}_{\text{em}}(\mathbf{r})$ , where  $\mathbf{A}_B(\mathbf{r})$  and  $\mathbf{A}_{\text{em}}(\mathbf{r})$  are vector potentials of the stationary magnetic field and electromagnetic wave, respectively. The interaction operator is  $H_{\text{int}} = H - H_0$ , where  $H_0$  is obtained from  $H$  by setting  $\mathbf{A}_{\text{em}}(\mathbf{r}) = 0$ . The unperturbed Hamiltonian  $H_0$  is responsible for the stationary states of He, discussed in Section 2. The vector potential and the wavefunctions may be subject to gauge transformations; the wavefunctions presented in Section 2 correspond to the cylindrical gauge  $\mathbf{A}_B(\mathbf{r}) = \frac{1}{2}\mathbf{B} \times \mathbf{r}$ . Neglecting non-linear (quadratic in  $\mathbf{A}_{\text{em}}$ ) term, we have

$$H_{\text{int}} \approx \frac{e}{2m_e c} \sum_{j=1,2} [\boldsymbol{\pi}_j \cdot \mathbf{A}_{\text{em}}(\mathbf{r}_j) + \mathbf{A}_{\text{em}}(\mathbf{r}_j) \cdot \boldsymbol{\pi}_j], \quad (20)$$

where

$$\boldsymbol{\pi} = \mathbf{p} + \frac{e}{c} \mathbf{A}_B(\mathbf{r}) \quad (21)$$

is the non-perturbed kinetic momentum operator:  $\boldsymbol{\pi} = m_e \dot{\mathbf{r}} = m_e (i/\hbar)[H_0 \mathbf{r} - \mathbf{r} H_0]$ .

For a monochromatic wave of the form  $\mathbf{A}_{\text{em}}(\mathbf{r}) \propto \boldsymbol{\epsilon} e^{i\mathbf{q}\cdot\mathbf{r}}$ , where  $\boldsymbol{\epsilon}$  is the unit polarization vector, applying the Fermi's Golden Rule and assuming the transverse polarization ( $\boldsymbol{\epsilon} \cdot \mathbf{q} = 0$ ), one obtains the following general formula for the cross-section of absorption of radiation from a given initial state  $|a\rangle$  (see e.g. Armstrong & Nicholls 1972):

$$\sigma(\omega, \boldsymbol{\epsilon}) = \sum_b \frac{4\pi^2}{\omega c} |\boldsymbol{\epsilon} \cdot \langle b | e^{i\mathbf{q}\cdot\mathbf{r}} \mathbf{j} | a \rangle|^2 \delta(\omega - \omega_{ba}), \quad (22)$$

where  $|b\rangle$  is the final state,  $\omega = qc$  is the photon frequency,  $\omega_{ba} = (E_b - E_a)/\hbar$  and  $\mathbf{j}$  is the electric current operator. In our case,  $\mathbf{j} = (-e/m_e)(\boldsymbol{\pi}_1 + \boldsymbol{\pi}_2)$ .

We will calculate the cross-sections in the dipole approximation – i.e. drop  $e^{i\mathbf{q}\cdot\mathbf{r}}$  from equation (22). This approximation is sufficiently accurate for the calculation of the total cross-section as long as  $\hbar\omega \ll m_e c^2$  (cf. e.g. Potekhin & Pavlov 1993, 1997 for the case of

H atom). In the dipole approximation, equation (22) can be written as

$$\sigma(\omega, \boldsymbol{\epsilon}) = \sum_b \frac{2\pi^2 e^2}{m_e c} f_{ba} \delta(\omega - \omega_{ba}), \quad (23)$$

where

$$f_{ba} = \frac{2}{\hbar\omega_{ba} m_e} |\langle b | \boldsymbol{\epsilon} \cdot \boldsymbol{\pi} | a \rangle|^2 = \frac{2m_e \omega_{ba}}{\hbar} |\langle b | \boldsymbol{\epsilon} \cdot \mathbf{r} | a \rangle|^2 \quad (24)$$

is the oscillator strength. In the second equality, we have passed from the ‘velocity form’ to the ‘length form’ of the matrix element (cf. e.g. Chandrasekhar 1945). These representations are identical for the exact wavefunctions, but it is not so for approximate ones. In the adiabatic approximation, the length representation (i.e. the right-hand side of equation 24) is preferable (see Potekhin & Pavlov 1993; Potekhin, Pavlov & Ventura 1997).

To evaluate the matrix element, we decompose the unit polarization vector  $\boldsymbol{\epsilon}$  into three cyclic components,

$$\boldsymbol{\epsilon} = \boldsymbol{\epsilon}_- \hat{\boldsymbol{e}}_+ + \boldsymbol{\epsilon}_+ \hat{\boldsymbol{e}}_- + \boldsymbol{\epsilon}_0 \hat{\boldsymbol{e}}_0, \quad (25)$$

with  $\hat{\boldsymbol{e}}_0 = \hat{\boldsymbol{e}}_z$  along the external magnetic field direction (the  $z$ -axis),  $\hat{\boldsymbol{e}}_{\pm} = (\hat{\boldsymbol{e}}_x \pm i\hat{\boldsymbol{e}}_y)/\sqrt{2}$  and  $\boldsymbol{\epsilon}_{\alpha} = \hat{\boldsymbol{e}}_{\alpha} \cdot \boldsymbol{\epsilon}$  (with  $\alpha = \pm, 0$ ). Then we can write the cross-section as the sum of three components,

$$\sigma(\omega, \boldsymbol{\epsilon}) = \sigma_+(\omega) |\boldsymbol{\epsilon}_+|^2 + \sigma_-(\omega) |\boldsymbol{\epsilon}_-|^2 + \sigma_0(\omega) |\boldsymbol{\epsilon}_0|^2, \quad (26)$$

where  $\sigma_{\alpha}$  has the same form as equation (23), with the corresponding oscillator strength given by

$$f_{ba}^{\alpha} = \frac{2m_e \omega_{ba} \rho_0^2}{\hbar} |M_{ba}|^2 = \frac{2\omega_{ba}}{\omega_c} |M_{ba}|^2, \quad (27)$$

with

$$M_{ba} = \langle b | \hat{\boldsymbol{e}}_{\alpha}^* \cdot \bar{\mathbf{r}} | a \rangle, \quad (28)$$

where  $\bar{\mathbf{r}} = \mathbf{r}/\rho_0$  and  $\omega_c = eB/(m_e c)$  is the electron cyclotron frequency.

#### 3.1 Bound-bound transitions

Consider the electronic transition

$$|a\rangle = |m\nu, m_2\nu_2\rangle = |W_m f_{m\nu}, W_{m_2} f_{m_2\nu_2}\rangle \\ \rightarrow |b\rangle = |m'\nu', m_2\nu_2\rangle = |W_{m'} g_{m'\nu'}, W_{m_2} g_{m_2\nu_2}\rangle. \quad (29)$$

The selection rules for allowed transitions and the related matrix elements are

$$\sigma_0 : \Delta m = 0, \Delta\nu = \text{odd}, \\ M_{ba} = \langle g_{m'\nu'} | \bar{z} | f_{m\nu} \rangle \langle g_{m_2\nu_2} | f_{m_2\nu_2} \rangle, \quad (30)$$

$$\sigma_+ : \Delta m = 1, \Delta\nu = \text{even}, \\ M_{ba} = \sqrt{m+1} \langle g_{m'\nu'} | f_{m\nu} \rangle \langle g_{m_2\nu_2} | f_{m_2\nu_2} \rangle, \quad (31)$$

$$\sigma_- : \Delta m = -1, \Delta\nu = \text{even}, \\ M_{ba} = \sqrt{m} \langle g_{m'\nu'} | f_{m\nu} \rangle \langle g_{m_2\nu_2} | f_{m_2\nu_2} \rangle, \quad (32)$$

where  $\Delta m = m' - m$ ,  $\Delta\nu = \nu' - \nu$ . The oscillator strengths for bound-bound transitions from the states  $|00, 10\rangle$  and  $|00, 20\rangle$  are given in Table 1.

The selection rules (30)–(32) are exact in the dipole approximation. The selection rules in  $m$  follow from the conservation of the  $z$ -projection of total (for the photon and two electrons) angular momentum. Technically, in the adiabatic approximation, they follow from the properties of the Landau functions (e.g. Potekhin & Pavlov

**Table 1.** Bound–bound transitions  $|a\rangle \rightarrow |b\rangle$ : the photon energy  $\hbar\omega_{ba} = E_b - E_a$  (in eV) and the oscillator strength  $f_{ba}^\alpha$  for different polarization components  $\alpha$  (see equation 27). All transitions  $\Delta\nu \leq 1$  from the initial states  $|00, 10\rangle$  and  $|00, 20\rangle$  are listed, for several magnetic field strengths  $B_{12} = B/(10^{12} \text{ G})$ . The last two columns list the transition energies  $\hbar\omega_{ba}^*$  and oscillator strengths  $f_{ba}^*$ , corrected for the finite mass of the nucleus, according to Section 5.1.

$B_{12}$	$\sigma$	$ a\rangle$	$\rightarrow  b\rangle$	$\hbar\omega_{ba}$	$f_{ba}$	$\hbar\omega_{ba}^*$	$f_{ba}^*$
1	0	$ 00, 10\rangle$	$\rightarrow  00, 11\rangle$	147.5	0.234	–	–
			$\rightarrow  10, 01\rangle$	271.8	0.124	–	–
	+	$ 00, 20\rangle$	$\rightarrow  00, 20\rangle$	43.11	0.0147	44.70	0.0153
			$\rightarrow  00, 21\rangle$	104.4	0.312	–	–
			$\rightarrow  20, 01\rangle$	277.7	0.115	–	–
			$\rightarrow  00, 30\rangle$	18.01	0.00930	19.60	0.0101
5	0	$ 00, 10\rangle$	$\rightarrow  00, 11\rangle$	256.2	0.127	–	–
			$\rightarrow  10, 01\rangle$	444.8	0.0603	–	–
	+	$ 00, 20\rangle$	$\rightarrow  00, 20\rangle$	66.95	0.00459	74.89	0.00512
			$\rightarrow  00, 21\rangle$	189.2	0.176	–	–
			$\rightarrow  20, 01\rangle$	455.0	0.0537	–	–
			$\rightarrow  00, 30\rangle$	28.94	0.00299	36.88	0.00381
10	0	$ 00, 10\rangle$	$\rightarrow  00, 11\rangle$	151.1	0.00512	159.0	0.00539
			$\rightarrow  10, 01\rangle$	318.9	0.0974	–	–
	+	$ 00, 20\rangle$	$\rightarrow  00, 20\rangle$	540.8	0.0457	–	–
			$\rightarrow  00, 21\rangle$	79.54	0.00273	95.42	0.00327
			$\rightarrow  20, 01\rangle$	239.4	0.136	–	–
			$\rightarrow  00, 30\rangle$	553.3	0.0405	–	–
50	0	$ 00, 10\rangle$	$\rightarrow  00, 11\rangle$	34.84	0.00179	50.72	0.00261
			$\rightarrow  10, 01\rangle$	177.0	0.00301	192.9	0.00328
	+	$ 00, 20\rangle$	$\rightarrow  00, 20\rangle$	510.9	0.0557	–	–
			$\rightarrow  00, 21\rangle$	822.2	0.0266	–	–
			$\rightarrow  20, 01\rangle$	114.2	7.85e–4	193.6	0.00133
			$\rightarrow  00, 30\rangle$	396.7	0.0776	–	–
100	0	$ 00, 10\rangle$	$\rightarrow  00, 11\rangle$	841.1	0.0235	–	–
			$\rightarrow  10, 01\rangle$	51.92	5.37e–4	131.3	0.00136
	+	$ 00, 20\rangle$	$\rightarrow  00, 20\rangle$	246.5	8.41e–4	325.9	0.00111
			$\rightarrow  00, 21\rangle$	616.4	0.0452	–	–
			$\rightarrow  20, 01\rangle$	971.4	0.0221	–	–
			$\rightarrow  00, 30\rangle$	131.4	4.52e–4	290.2	9.98e–4
+	$ 00, 20\rangle$	$\rightarrow  00, 21\rangle$	485.0	0.0626	–	–	
		$\rightarrow  20, 01\rangle$	993.4	0.0195	–	–	
+	$ 00, 20\rangle$	$\rightarrow  00, 30\rangle$	60.57	3.13e–4	219.4	0.00114	
		$\rightarrow  20, 10\rangle$	280.7	4.80e–4	439.5	7.51e–4	

1993). The selection rules in  $\nu$  follow from the fact that the functions  $g_{m'\nu'}$  and  $f_{m\nu}$  have the same parity for even  $\nu' - \nu$  and opposite parity for odd  $\nu' - \nu$ .

In addition to these selection rules, there are approximate selection rules which rely on the approximate orthogonality of functions  $g_{m'\nu'}$  and  $f_{m\nu}$  (for general  $\nu \neq \nu'$ ). Because of this approximate orthogonality, which holds better the larger  $B$  is, we have

$$\langle g_{m'\nu'} | f_{m\nu} \rangle \langle g_{m_2\nu_2} | f_{m_2\nu_2} \rangle = \delta_{\nu,\nu'} + \varepsilon, \quad (33)$$

where  $|\varepsilon| \ll 1$  and  $\varepsilon \rightarrow 0$  as  $\Delta\nu \rightarrow \pm\infty$ . Therefore, the oscillator strengths for transitions with  $\alpha = \pm$  and  $\Delta\nu = 2, 4, \dots$  are small compared to those with  $\Delta\nu = 0$ . The latter oscillator strengths can be approximated, according to equations (27), (31), (32) and (33), by

$$f_{ba}^+ \approx 2(m+1)\omega_{ba}/\omega_c, \quad f_{ba}^- \approx 2m\omega_{ba}/\omega_c \quad (34)$$

( $\alpha = \Delta m = \pm 1, \nu' = \nu$ ).

The same approximate orthogonality leads to the smallness of matrix elements for transitions of the type  $|m\nu, m_2\nu_2\rangle \rightarrow |m'\nu', m_2\nu_2'\rangle$  with  $\nu_2' \neq \nu_2$  for  $\alpha = \pm$  and the smallness of cross terms in the matrix elements of the form  $\langle g_{m_2\nu_2} | f_{m\nu} \rangle \langle g_{m'\nu'} | f_{m_2\nu_2'} \rangle$  when  $m' = m_2$  (i.e. the so-called ‘one-electron jump rule’); we have

therefore excluded such terms from the selection rule equations above (equations 30–32).

### 3.2 Photoionization

The bound–free absorption cross-section for the transition from the bound state  $|b\rangle$  to the continuum state  $|f\rangle$  is given by equation (22) with obvious substitutions  $|a\rangle \rightarrow |b\rangle, |b\rangle \rightarrow |f\rangle$  and

$$\sum_f \rightarrow (L_z/2\pi) \int_{-\infty}^{\infty} dk, \quad (35)$$

where  $L_z$  is the normalization length of the continuum electron [ $\int_{-L_z/2}^{L_z/2} dz |g_{mk}(z)|^2 = 1$ ] and  $k$  is the wavenumber of the outgoing electron (Section 2.2). Therefore, we have

$$\sigma_{\text{bf}}(\omega, \epsilon) = \frac{2\pi e^2 L_z}{m_e c \hbar^2 \omega_{fb} k} \left\{ \left| \langle f_{\pm k} | e^{iq \cdot r} \epsilon \cdot \pi | b \rangle \right|^2 + \left| \langle f_{\mp k} | e^{iq \cdot r} \epsilon \cdot \pi | b \rangle \right|^2 \right\}, \quad (36)$$

where  $k = \sqrt{2m_e \epsilon_f}/\hbar$  and  $|f_{\pm k}\rangle$  represents the final state where the free electron has wavenumber  $\pm k$  (here and hereafter we

assume  $k > 0$ ). The asymptotic conditions for these outgoing free electrons are (cf. e.g. Potekhin et al. 1997)  $g_{mk}(z) \sim \exp[i\varphi_k(z)]$  at  $z \rightarrow \pm\infty$ , where  $\varphi_k(z) = |kz| + (ka_0)^{-1} \ln |kz|$  and  $a_0 = \hbar^2/m_e e^2$  is the Bohr radius. Since we do not care about direction of the outgoing electron, we can use for calculations a basis of symmetric and antisymmetric wavefunctions of the continuum – that is, in equation (36) we can replace  $\langle f_k |$  and  $\langle f_{-k} |$  by  $\langle f_{\text{even}} |$  and  $\langle f_{\text{odd}} |$ . The symmetric state  $|f_{\text{even}}\rangle$  is determined by the free electron boundary condition  $g'_{mk,\text{even}}(0) = 0$  and the antisymmetric state  $|f_{\text{odd}}\rangle$  is determined by  $g_{mk,\text{odd}}(0) = 0$ . Since the coefficients in equation (17) are real,  $g_{mk,\text{even}}(z)$  and  $g_{mk,\text{odd}}(z)$  can be chosen real. At  $z \rightarrow \pm\infty$ , they behave as  $g_{mk,(\text{even},\text{odd})}(z) \sim \sin[\varphi(z) + \text{constant}]$  (where the value of constant depends on all quantum numbers, including  $k$ ). We still have the normalization  $\int_{-L_z/2}^{L_z/2} dz |g_{mk,(\text{even},\text{odd})}(z)|^2 = 1$ .

Similar to bound–bound transitions, we can decompose the bound–free cross-section into three components (equation 26). Thus, using the dipole approximation and the length form of the matrix elements, as discussed above, we have for  $(\alpha = \pm, 0)$ -components of the bound–free cross-section

$$\sigma_{\text{bf},\alpha}(\omega) = \frac{3}{4} \sigma_{\text{Th}} \left( \frac{m_e c^2}{\hbar \omega} \right)^3 \sqrt{\frac{m_e c^2}{2\varepsilon_f}} \left( \frac{L_z a_0}{\rho_0^2} \right) \left( \frac{\omega \rho_0}{c} \right)^4 \times |\langle f | \hat{e}_\alpha^* \cdot \vec{r} | b \rangle|^2, \quad (37)$$

where  $|f\rangle = |f_{\text{even}}\rangle$  or  $|f\rangle = |f_{\text{odd}}\rangle$  depending on the parity of the initial state and according to the selection rules, and  $\sigma_{\text{Th}} = (8\pi/3)(e^2/m_e c^2)^2$  is the Thomson cross-section. The selection rules and related matrix elements for the bound–free transitions

$$|b\rangle = |m\nu, m_2\nu_2\rangle = |W_m f_{m\nu}, W_{m_2} f_{m_2\nu_2}\rangle \\ \rightarrow |f\rangle = |m'k, m_2\nu_2\rangle = |W_{m'} g_{m'k}, W_{m_2} g_{m_2\nu_2}\rangle \quad (38)$$

are similar to those for the bound–bound transitions (see equations 30–32):

$$\sigma_0 : \Delta m = 0, \Delta\nu = \text{odd}, \\ M_{fb} = \langle g_{mk} | \vec{z} | f_{m\nu} \rangle \langle g_{m_2\nu_2} | f_{m_2\nu_2} \rangle, \quad (39)$$

$$\sigma_+ : \Delta m = 1, \Delta\nu = \text{even}, \\ M_{fb} = \sqrt{m+1} (\langle g_{m'k} | f_{m\nu} \rangle \langle g_{m_2\nu_2} | f_{m_2\nu_2} \rangle \\ - \delta_{m'v, m_2\nu_2} \langle g_{m_2\nu_2} | f_{m\nu} \rangle \langle g_{m'k} | f_{m_2\nu_2} \rangle), \quad (40)$$

$$\sigma_- : \Delta m = -1, \Delta\nu = \text{even}, \\ M_{fb} = \sqrt{m} (\langle g_{m'k} | f_{m\nu} \rangle \langle g_{m_2\nu_2} | f_{m_2\nu_2} \rangle \\ - \delta_{m'v, m_2\nu_2} \langle g_{m_2\nu_2} | f_{m\nu} \rangle \langle g_{m'k} | f_{m_2\nu_2} \rangle), \quad (41)$$

In this case, the condition  $\Delta\nu = \text{odd}$  means that  $g_{m'k}$  and  $f_{m\nu}$  must have opposite parity, and the condition  $\Delta\nu = \text{even}$  means that  $g_{m'k}$  and  $f_{m\nu}$  must have the same parity. The oscillator strengths for bound–free transitions from the states  $|00, 10\rangle$  and  $|00, 20\rangle$  are given in Table 2.

Note that in equations (40) and (41), the second term in the matrix element (of the form  $\langle g_{m_2\nu_2} | f_{m\nu} \rangle \langle g_{m'k} | f_{m_2\nu_2} \rangle$ ) corresponds to transitions of both electrons. This appears to violate the ‘one-electron jump rule’ and other approximate selection rules discussed in Section 3.1 (see equation 33). In fact, these approximate rules are not directly relevant for bound–free transitions, since the matrix elements involving a continuum state are always small:  $\langle g_{m'k} | f_{m\nu} \rangle \rightarrow 0$  as the normalization length  $L_z \rightarrow \infty$ . Rather, we use a different set of

selection rules to determine which of these ‘small’ matrix elements are smaller than the rest. The first is that

$$\langle g_{m'k} | f_{m\nu} \rangle \langle g_{m_2\nu_2} | f_{m_2\nu_2} \rangle \gg \langle g_{m'k} | f_{m\nu} \rangle \langle g_{m_2\nu'_2} | f_{m_2\nu_2} \rangle, \quad (42)$$

when  $\nu'_2 \neq \nu_2$ . This selection rule is similar to the bound–bound transition case as  $\langle g_{m_2\nu'_2} | f_{m_2\nu_2} \rangle$  involves a bound electron transition, not a free electron transition. The second approximate selection rule that applies here is more complicated: terms of the form  $\langle g_{m'v} | f_{m\nu} \rangle \langle g_{m_2k} | f_{m_2\nu_2} \rangle$  are small, unless  $m' = m_2$  and  $\nu_2 = \nu$ . This exception for  $m' = m_2$  and  $\nu_2 = \nu$  is due to the exchange term in the differential equation for the free electron wavefunction (equation 17), which strongly (anti)correlates the two final wavefunctions  $|g_{m'v}\rangle$  and  $|g_{m_2k}\rangle$ . If  $m' = m_2$  and  $\nu = \nu_2$ , then since  $\langle g_{m'v} | f_{m_2\nu_2} \rangle$  is not small (in fact, it is of the order of 1),  $\langle g_{m_2k} | f_{m_2\nu_2} \rangle$  will not be small but will be of the same order as other terms involving the free electron wavefunction. In particular, the second selection rule means, e.g., that the matrix element for the transition from  $|00, 10\rangle$  to  $|00, 0k\rangle$  is

$$M_{00,10 \rightarrow 00,0k} = \langle g_{0k} | f_{10} \rangle \langle g_{00} | f_{00} \rangle - \langle g_{00} | f_{10} \rangle \langle g_{0k} | f_{00} \rangle, \quad (43)$$

where the second term is non-negligible, but that the matrix element for the transition from  $|00, 10\rangle$  to  $|0k, 20\rangle$ , which is

$$M_{00,10 \rightarrow 0k,20} = \langle g_{20} | f_{10} \rangle \langle g_{0k} | f_{00} \rangle, \quad (44)$$

is small compared to the other matrix elements and can be ignored (see Fig. 1).

We make one final comment here about the effect of exchange interaction on the free electron state. If the exchange term (the right-hand side of equation 17) is neglected in the calculation of the free electron wavefunction, then the cross terms (i.e. those involving two-electron transitions) in the matrix elements of equations (40) and (41) are small and can be neglected. One then obtains approximate photoionization cross-sections which are within a factor of 2 of the true values in most cases and much better for  $\sigma_0$  transitions. If the exchange term is included in equation (17) but the cross terms in the matrix elements are ignored, significant errors in the  $\sigma_\pm$  photoionization cross-sections will result. To obtain reliable cross-sections for all cases, both the exchange effect on the free electron and the contribution of two-electron transitions must be included.

## 4 RESULTS

Tables 1 and 2 give results for transitions of helium atoms from the ground state  $(|00, 10\rangle)$  and the first excited state  $(|00, 20\rangle)$ . Table 1 gives results (photon energies and oscillator strengths) for all possible bound–bound transitions with  $\Delta\nu \leq 1$ , for the field strengths  $B_{12} = 1, 5, 10, 50, 100$ , where  $B_{12} = B/(10^{12} \text{ G})$ . Transitions  $|a\rangle \rightarrow |b\rangle$  for  $\alpha = -$  are not listed separately, being equivalent to transitions  $|b\rangle \rightarrow |a\rangle$  for  $\alpha = +$ . One can check that the oscillator strengths  $f_{ba}$  presented in Table 1 for  $\alpha = +$  are well described by the approximation (34).

Table 2 gives results (threshold photon energies and cross-section fitting formulae, see below) for all possible bound–free transitions. Figure 1 shows partial cross-section curves for all bound–free transitions from the ground state of helium for  $B_{12} = 1$ . The transition  $|00, 10\rangle \rightarrow |0k, 20\rangle$  is an example of a ‘weak’ transition, whose oscillator strength is small because of the approximate orthogonality of one-electron wavefunctions, as discussed at the end of Section 3.1. It is included in this figure to confirm the accuracy of our assumption. Figs 2 and 3 show total cross-section curves for a photon polarized along the magnetic field, for  $B_{12} = 1$  and 100, respectively.

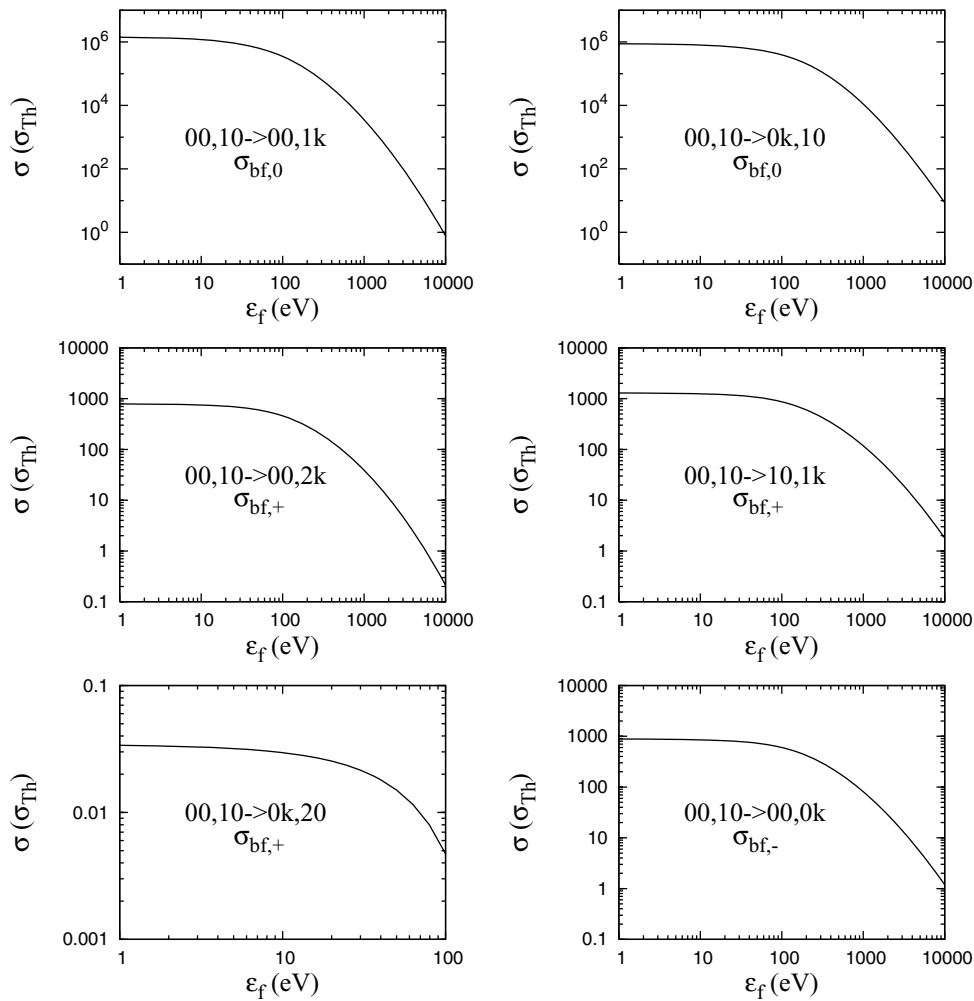


**Figure 1.** Partial cross-sections  $\sigma_{(0,+,-)}$  versus final ionized electron energy for photoionization of the ground state helium atom  $((m_1, m_2) = (1, 0))$ . The field strength is  $10^{12}$  G. The transition  $|00, 10\rangle \rightarrow |0k, 20\rangle$  in the bottom left panel is an example of a ‘weak’ transition. We have ignored these transitions in our calculations of the total cross-sections.

Figs 4 and 5 show total cross-sections for the circular polarizations,  $\alpha = \pm$ , for  $B_{12} = 1$ . Finally, Figs 6 and 7 show total cross-sections for  $\alpha = \pm$  and  $B_{12} = 100$ .

#### 4.1 Fitting formula

The high-energy cross-section scaling relations from Potekhin & Pavlov (1993), which were derived for hydrogen photoionization in strong magnetic fields, also hold for helium:

$$\sigma_{\text{bf},0} \propto \left(\frac{1}{\hbar\omega}\right)^{2m_i+9/2} \quad (45)$$

$$\sigma_{\text{bf},\pm} \propto \left(\frac{1}{\hbar\omega}\right)^{2m_i+7/2}, \quad (46)$$

where  $m_i$  is the  $m$  value of the initial electron that transitions to the free state. In addition, we use similar fitting formulae for our numerical cross-sections:

$$\sigma_{\text{bf},0} \simeq \frac{\mathcal{C}}{(1 + \mathcal{A}y)^{2.5}(1 + \mathcal{B}(\sqrt{1+y} - 1))^{4(m_i+1)}} \sigma_{\text{Th}} \quad (47)$$

$$\sigma_{\text{bf},\pm} \simeq \frac{\mathcal{C}(1+y)}{(1 + \mathcal{A}y)^{2.5}(1 + \mathcal{B}(\sqrt{1+y} - 1))^{4(m_i+1)}} \sigma_{\text{Th}} \quad (48)$$

where  $y = \varepsilon_f/\hbar\omega_{\text{thr}}$  and  $\hbar\omega_{\text{thr}}$  is the threshold photon energy for photoionization. These formulae have been fit to the cross-section curves with respect to the free electron energy  $\varepsilon_f$  in approximately the  $1-10^4$  eV range (the curves are fit up to  $10^5$  eV for strong magnetic fields  $B_{12} = 50-100$ , in order to obtain the appropriate high-energy factor). The data points to be fit are weighted proportional to their cross-section values plus a slight weight toward low-energy values, according to the formula (error in  $\sigma$ )  $\propto \sigma \varepsilon_f^{0.25}$ .

Results for the three fitting parameters,  $\mathcal{A}$ ,  $\mathcal{B}$  and  $\mathcal{C}$ , are given in Table 2 for various partial cross-sections over a range of magnetic field strengths. For photoionization in strong magnetic fields ( $B_{12} \gtrsim 50$ ), the cross-section curves we generate for the  $\sigma_+$  and  $\sigma_-$  transitions have a slight deficiency at low electron energies, such that the curves peak at  $\varepsilon_f \simeq 10$  eV, rather than at threshold as expected. These peaks do not represent a real effect, but rather reflect the limits on the accuracy of our code (the overlap of the wavefunction of the transitioning electron pre- and post-ionization is extremely small under these conditions). Because the cross-section values are not correct at low energies, our fits are not as accurate for these curves. In Table 2, we have marked with a ‘\*’ those transitions which are

**Table 2.** Bound-free transitions  $|b\rangle \rightarrow |f\rangle$ : the threshold photon energy  $\hbar\omega_{\text{thr}}$  (in eV) and the fitting parameters  $\mathcal{A}$ ,  $\mathcal{B}$  and  $\mathcal{C}$  used in the cross-section fitting formulae (equation 48). All transitions from the initial states  $|00, 10\rangle$  and  $|00, 20\rangle$  are listed, for several magnetic field strengths  $B_{12} = B/(10^{12} \text{ G})$ .

$B_{12}$	$\sigma$	$ b\rangle$	$\rightarrow  f\rangle$	$m_i$	$\hbar\omega_{\text{thr}}$	$A$	$B$	$C$		
1	0	$ 00, 10\rangle$	$\rightarrow  00, 1k\rangle$	1	159.2	0.96	0.093	1.43e6		
			$\rightarrow  10, 0k\rangle$	0	283.2	0.89	0.20	8.83e5		
			$\rightarrow  00, 2k\rangle$	1	159.2	0.70	0.061	7.95e2		
			$\rightarrow  10, 1k\rangle$	0	283.2	0.86	0.094	1.30e3		
			$\rightarrow  00, 0k\rangle$	1	159.2	0.62	0.030	8.89e2		
			$\rightarrow  00, 2k\rangle$	2	116.0	1.00	0.062	1.78e6		
	+	$ 00, 20\rangle$	$\rightarrow  20, 0k\rangle$	0	289.2	0.88	0.22	8.71e5		
			$\rightarrow  00, 3k\rangle$	2	116.0	0.66	0.038	3.94e2		
			$\rightarrow  20, 1k\rangle$	0	289.2	0.54	0.14	6.48e2		
			$\rightarrow  00, 1k\rangle$	2	116.0	0.62	0.029	5.82e2		
			-	$ 00, 10\rangle$	$\rightarrow  00, 1k\rangle$	1	268.2	0.86	0.061	8.39e5
					$\rightarrow  10, 0k\rangle$	0	456.4	0.69	0.16	4.60e5
$\rightarrow  00, 2k\rangle$	1	268.2			0.68	0.036	1.14e2			
$\rightarrow  10, 1k\rangle$	0	456.4			0.83	0.057	1.93e2			
$\rightarrow  00, 0k\rangle$	1	268.2			0.60	0.020	1.36e2			
$\rightarrow  00, 2k\rangle$	2	201.2			0.92	0.039	1.11e6			
5	0	$ 00, 20\rangle$	$\rightarrow  20, 0k\rangle$	0	466.5	0.65	0.18	4.39e5		
			$\rightarrow  00, 3k\rangle$	2	201.2	0.65	0.021	5.95e1		
			$\rightarrow  20, 1k\rangle$	0	466.5	0.54	0.084	9.13e1		
			$\rightarrow  00, 1k\rangle$	2	201.2	0.61	0.015	7.82e1		
			+	$ 00, 10\rangle$	$\rightarrow  00, 1k\rangle$	1	331.1	0.82	0.051	6.58e5
					$\rightarrow  10, 0k\rangle$	0	552.5	0.63	0.15	3.51e5
	$\rightarrow  00, 2k\rangle$	1			331.1	0.67	0.029	4.94e1		
	$\rightarrow  10, 1k\rangle$	0			552.5	0.81	0.046	8.43e1		
	$\rightarrow  00, 0k\rangle$	1			331.1	0.59	0.016	6.00e1		
	$\rightarrow  00, 2k\rangle$	2			251.6	0.88	0.033	8.77e5		
	10	0	$ 00, 20\rangle$	$\rightarrow  20, 0k\rangle$	0	564.9	0.59	0.16	3.31e5	
				$\rightarrow  00, 3k\rangle$	2	251.6	0.64	0.017	2.64e1	
$\rightarrow  20, 1k\rangle$				0	564.9	0.53	0.069	3.97e1		
$\rightarrow  00, 1k\rangle$				2	251.6	0.61	0.012	3.25e1		
+				$ 00, 10\rangle$	$\rightarrow  00, 1k\rangle$	1	523.3	0.73	0.034	3.74e5
					$\rightarrow  10, 0k\rangle$	0	834.2	0.54	0.11	1.96e5
		$\rightarrow  00, 2k\rangle$	1		523.3	0.63	0.020	7.15e0		
		$\rightarrow  10, 1k\rangle$	0		834.2	0.77	0.033	1.22e1		
		$\rightarrow  00, 0k\rangle$	1		523.3	0.57	0.012	8.94e0		
		$\rightarrow  00, 2k\rangle$	2		409.1	0.79	0.021	5.02e5		
50		0	$ 00, 20\rangle$	$\rightarrow  20, 0k\rangle$	0	853.0	0.50	0.13	1.83e5	
				$\rightarrow  00, 3k\rangle$	2	409.1	0.62	0.0104	4.04e0	
	$\rightarrow  20, 1k\rangle$			0	853.0	*0.52	0.052	5.88e0		
	$\rightarrow  00, 1k\rangle$			2	409.1	0.59	0.0058	4.13e0		
	+			$ 00, 10\rangle$	$\rightarrow  00, 1k\rangle$	1	628.8	0.69	0.029	2.96e5
					$\rightarrow  10, 0k\rangle$	0	983.4	0.51	0.101	1.56e5
		$\rightarrow  00, 2k\rangle$	1		628.8	0.62	0.019	3.12e0		
		$\rightarrow  10, 1k\rangle$	0		983.4	0.75	0.031	5.33e0		
		$\rightarrow  00, 0k\rangle$	1		628.8	0.56	0.012	3.94e0		
		$\rightarrow  00, 2k\rangle$	2		498.0	0.75	0.018	3.96e5		
	100	0	$ 00, 20\rangle$	$\rightarrow  20, 0k\rangle$	0	1008	0.47	0.12	1.45e5	
				$\rightarrow  00, 3k\rangle$	2	498.0	0.60	0.0092	1.81e0	
$\rightarrow  20, 1k\rangle$				0	1008	*0.50	0.050	2.60e0		
$\rightarrow  00, 1k\rangle$				2	498.0	0.58	0.0042	1.69e0		
+				$ 00, 10\rangle$	$\rightarrow  00, 1k\rangle$	1	628.8	0.69	0.029	2.96e5
					$\rightarrow  10, 0k\rangle$	0	983.4	0.51	0.101	1.56e5
		$\rightarrow  00, 2k\rangle$	1		628.8	0.62	0.019	3.12e0		
		$\rightarrow  10, 1k\rangle$	0		983.4	0.75	0.031	5.33e0		
		$\rightarrow  00, 0k\rangle$	1		628.8	0.56	0.012	3.94e0		
		$\rightarrow  00, 2k\rangle$	2		498.0	0.75	0.018	3.96e5		

most inaccurately fit by our fitting formula, determined by cross-section curves with low-energy dips greater than 5 per cent of the threshold cross-section value.

## 5 FINITE NUCLEUS MASS EFFECTS

So far, we have used the infinite ion mass approximation. In this section, we will evaluate the validity range of this approximation and suggest possible corrections.

It is convenient to use the coordinate system which contains the centre-of-mass coordinate  $\mathbf{R}_{\text{cm}}$  and the relative coordinates  $\{r_j\}$  of the electrons with respect to the nucleus. Using a suitable canonical transformation, the Hamiltonian  $H$  of an arbitrary atom or ion can be separated into three terms (Vincke & Baye 1988; Baye & Vincke 1990; Schmelcher & Cederbaum 1991):  $H_1$  which describes the motion of a free pseudo-particle with net charge  $Q$  and total mass  $M$  of the ion (atom), the coupling term  $H_2$  between the collective and internal motion, and  $H_3$  which describes the internal relative motion

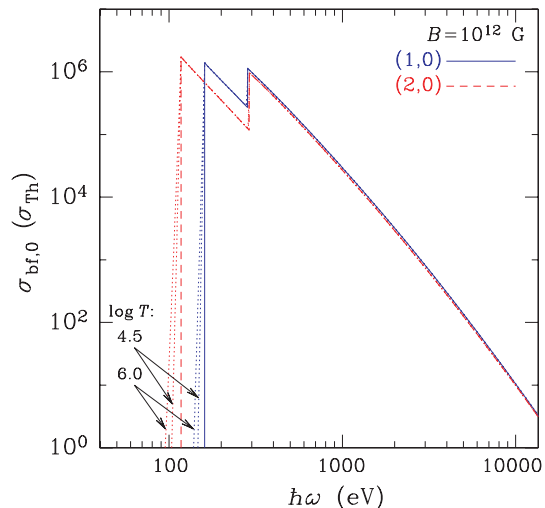


**Figure 2.** Total cross-section  $\sigma_0$  versus photon energy for helium photoionization, from initial states  $(m_1, m_2) = (1, 0)$  (solid lines) and  $(2, 0)$  (dashed lines). The field strength is  $10^{12}$  G. The dotted lines extending from each cross-section curve represent the effect of magnetic broadening on these cross-sections, as approximated in equation (55), for  $T = 10^{4.5}$  K (steeper lines) and  $10^6$  K (flatter lines).

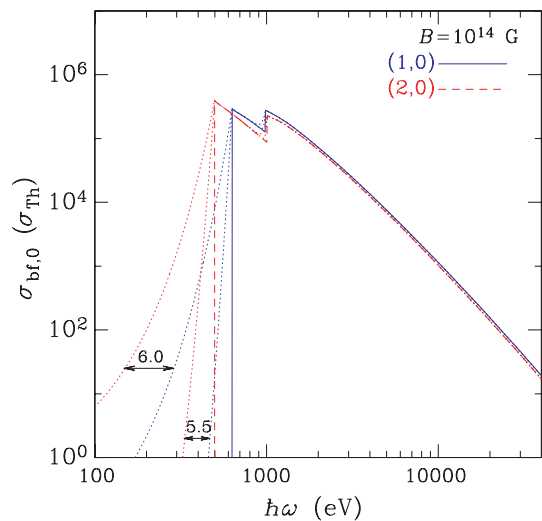


**Figure 3.** Total cross-section  $\sigma_0$  versus photon energy for helium photoionization, from initial states  $(m_1, m_2) = (1, 0)$  (solid lines) and  $(2, 0)$  (dashed lines). The field strength is  $10^{14}$  G. The dotted lines extending from each cross-section curve represent the effect of magnetic broadening on these cross-sections, as approximated in equation (55), for  $T = 10^{5.5}$  K (steeper lines) and  $10^6$  K (flatter lines).

of the electrons and the nucleus.  $H_1$  and  $H_2$  are proportional to  $M^{-1}$ , so they vanish in the infinite mass approximation. It is important to note, however, that  $H_3$  (the only non-zero term in the infinite mass approximation) also contains a term that depends on  $M_0^{-1}$ , where  $M_0 \approx M$  is the mass of the nucleus. Thus, there are two kinds of non-trivial finite-mass effects: the effects due to  $H_1 + H_2$ , which can be interpreted as caused by the electric field induced in the comoving reference frame, and the effects due to  $H_3$ , which arise irrespective of the atomic motion. Both kinds of effects have been included in calculations only for the H atom (Potekhin 1994; Potekhin & Pavlov 1997, and references therein) and  $\text{He}^+$  ion (Bezchastnov

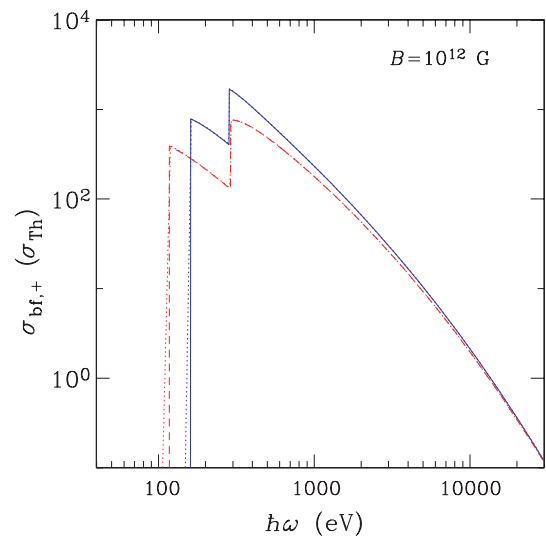


**Figure 4.** Total cross-section  $\sigma_+$  versus photon energy for helium photoionization, from initial states  $(m_1, m_2) = (1, 0)$  (solid lines) and  $(2, 0)$  (dashed lines). The field strength is  $10^{12}$  G. The dotted lines extending from each cross-section curve represent the effect of magnetic broadening on these cross-sections, as approximated in equation (55), for  $T = 10^6$  K.

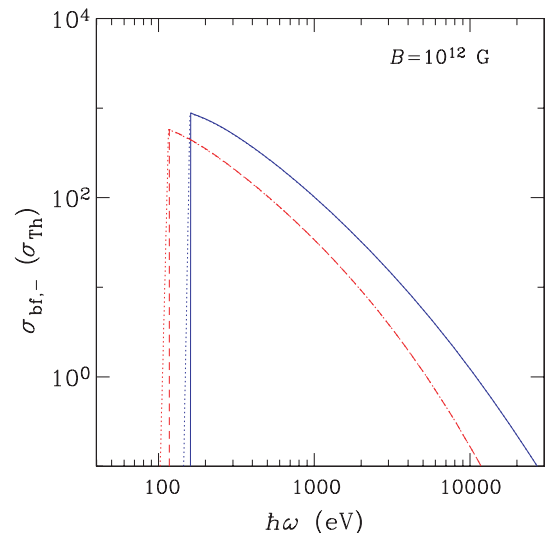


**Figure 5.** The same as in Fig. 4, but for  $\sigma_-$ .

et al. 1998; Pavlov & Bezchastnov 2005). For the He atom, only the second kind of effects have been studied (Al-Hujaj & Schmelcher 2003a,b).

### 5.1 Non-moving helium atom

The state of motion of an atom can be described by pseudo-momentum  $\mathbf{K}$ , which is a conserved vector since  $Q = 0$  (e.g. Vincke & Baye 1988; Schmelcher & Cederbaum 1991). Let us consider first the non-moving helium atom:  $K = 0$ .

According to Al-Hujaj & Schmelcher (2003a), there are trivial *normal mass corrections*, which consist in the appearance of reduced masses  $m_e/(1 \pm m_e/M_0)$  in  $H_3$ , and non-trivial *specific mass corrections*, which originate from the mass polarization operator.

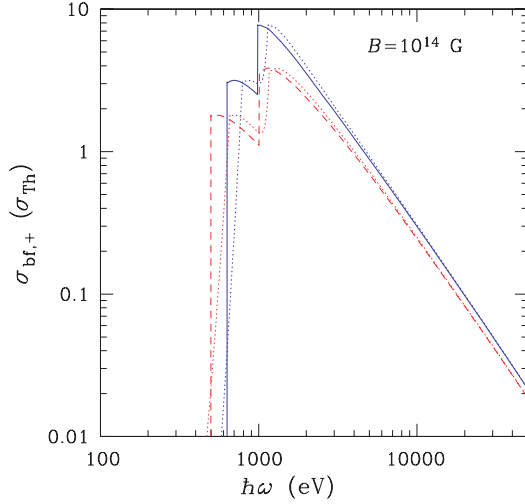


**Figure 6.** The same as in Fig. 4, but for  $B = 10^{14}$  G.

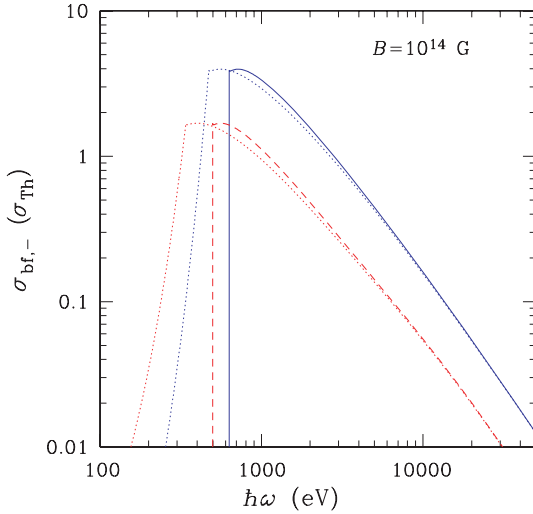


**Figure 7.** The same as in Fig. 6, but for  $\sigma_-$ .

The normal mass corrections for the total energy  $E$  of the He state  $|m_1\nu_1, m_2\nu_2\rangle$  can be described as follows:

$$E(M_0, B) = \frac{E(\infty, (1 + m_e/M_0)^2 B)}{1 + m_e/M_0} + \hbar\Omega_c \sum_j m_j, \quad (49)$$

where  $\Omega_c = (m_e/M_0)\omega_c$  (for He,  $\hbar\Omega_c = 1.588 B_{12}$  eV). The first term on the right-hand side describes the reduced mass transformation. The second term represents the energy shift due to conservation of the total  $z$  component of the angular momentum. Because of this shift, the states with sufficiently large values of  $m_1 + m_2$  become unbound (autoionizing, in analogy with the case of the H atom considered by Potekhin et al. 1997). This shift is also important for radiative transitions which change  $(m_1 + m_2)$  by  $\Delta m \neq 0$ : the transition energy  $\hbar\omega_{ba}$  is changed by  $\hbar\Omega_c \Delta m$ . The dipole matrix elements  $M_{ba}$  are only slightly affected by the normal mass corrections, but the oscillator strengths are changed with changing  $\omega_{ba}$  according to equation (27). The energy shift also leads to the splitting of the photoionization threshold by the same quantity  $\hbar\Omega_c \Delta m$ , with  $\Delta m = 0, \pm 1$  depending on the polarization (in the dipole approximation). Clearly, these corrections must be taken into account, unless

$\Omega_c \ll \omega_{ba}$  or  $\Delta m = 0$ , as illustrated in the last two columns of Table 1.

The specific mass corrections are more difficult to evaluate, but they can be neglected in the considered  $B$  range. Indeed, calculations by Al-Hujaj & Schmelcher (2003a) show that these corrections do not exceed 0.003 eV at  $B \leq 10^4 B_0$ .

## 5.2 Moving helium atom

Eigenenergies and wavefunctions of a moving atom depend on its pseudo-momentum  $\mathbf{K}$  perpendicular to the magnetic field. This dependence can be described by Hamiltonian components (e.g. Schmelcher & Cederbaum 1991)

$$H_1 + H_2 = \frac{K^2}{2M} + \sum_j \frac{e}{Mc} \mathbf{K} \cdot (\mathbf{B} \times \mathbf{r}_j), \quad (50)$$

where  $\sum_j$  is the sum over all electrons. The dependence on  $K_z$  is trivial, but the dependence on the perpendicular component  $K_\perp$  is not. The energies depend on the absolute value  $K_\perp$ . For calculation of radiative transitions, it is important to take into account that the pseudo-momentum of the atom in the initial and final state differs due to recoil:  $\mathbf{K}' = \mathbf{K} + \hbar\mathbf{q}$ . Effectively, the recoil adds a term  $\propto \mathbf{q}$  into the interaction operator (cf. Potekhin et al. 1997; Potekhin & Pavlov 1997). The recoil should be neglected in the dipole approximation.

The atomic energy  $E$  depends on  $K_\perp$  differently for different quantum states of the atom. In a real NS atmosphere, one should integrate the binding energies and cross-sections over the  $K_\perp$ -distribution of the atoms, in order to obtain the opacities.<sup>1</sup> Such integration leads to the specific magnetic broadening of spectral lines and ionization edges. Under the conditions typical for NS atmospheres, the magnetic broadening turns out to be much larger than the conventional Doppler and collisional broadenings (Pavlov & Potekhin 1995).

At present, the binding energies and cross-sections of a moving helium atom have not been calculated. However, we can approximately estimate the magnetic broadening for  $T \ll |(\Delta E)_{\min}|/k_B$ , where  $(\Delta E)_{\min}$  is the energy difference from a considered atomic level to the nearest level admixed by the perturbation due to atomic motion, and  $k_B$  is the Boltzmann constant. In this case, the  $K_\perp$ -dependence of  $E$  can be approximated by the formula

$$E(K_\perp) = E(0) + \frac{K_\perp^2}{2M_\perp}, \quad (51)$$

where  $E(0)$  is the energy in the infinite mass approximation and  $M_\perp = K_\perp(\partial E/\partial K_\perp)^{-1}$  is an effective ‘transverse’ mass, whose value ( $M_\perp > M$ ) depends on the quantum state considered (e.g. Vincke & Baye 1988; Pavlov & Mészáros 1993).

Generally, at every value of  $K_\perp$  one has a different cross-section  $\sigma(\omega, K_\perp)$ . Assuming the equilibrium (Maxwell–Boltzmann) distribution of atomic velocities, the  $K_\perp$ -averaged cross-section can be written as

$$\sigma(\omega) = \int_{E_{\min}}^{\infty} \exp\left(\frac{E(0) - E(K_\perp)}{k_B T}\right) \sigma(\omega, K_\perp) \frac{dE(K_\perp)}{k_B T}, \quad (52)$$

where  $E_{\min} = -\hbar\omega$ .

The transitions that were dipole-forbidden for an atom at rest due to the conservation of the total  $z$ -projection of angular momentum

<sup>1</sup> For the hydrogen atom, this has been done by Pavlov & Potekhin (1995) for bound–bound transitions and by Potekhin & Pavlov (1997) for bound–free transitions.

become allowed for a moving atom. Therefore, the selection rule  $\Delta m = \alpha$  (equations 30–32) does not strictly hold, and we must write

$$\sigma(\omega, K_{\perp}) = \sum_{m'} \sigma_{m'}(\omega, K_{\perp}), \quad (53)$$

where the sum of partial cross-sections is over all final quantum numbers  $m'$  (with  $m' \geq 0$  and  $m' \neq m_2$  for  $\Delta v = 0$ ) which are energetically allowed. For bound–bound transitions, this results in the splitting of an absorption line at a frequency  $\omega_{ba}$  in a multiplet at frequencies  $\omega_{ba} + \delta m \Omega_c + (M_{\perp, m'}^{-1} - M_{\perp}^{-1}) K_{\perp}^2 / 2\hbar$ , where  $\delta m \equiv m' - m - \alpha$  and  $M_{\perp, m'}$  is the transverse mass of final states. For photoionization, we have the analogous splitting of the threshold. In particular, there appear bound–free transitions at frequencies  $\omega < \omega_{\text{thr}}$  – they correspond to  $\delta m < K_{\perp}^2 / (2M_{\perp} \hbar \Omega_c)$ . Here,  $\omega_{\text{thr}}$  is the threshold in the infinite ion mass approximation, and one should keep in mind that the considered perturbation theory is valid for  $K_{\perp}^2 / 2M_{\perp} \ll |(\Delta E)_{\text{min}}| < \hbar \omega_{\text{thr}}$ . According to equation (53),  $\sigma(\omega, K_{\perp})$  is notched at  $\omega < \omega_{\text{thr}}$ , with the cogs at partial thresholds  $\omega_{\text{thr}} + \delta m \Omega_c - K_{\perp}^2 / (2M_{\perp} \hbar)$  (cf. fig. 2 in Potekhin & Pavlov 1997).

Let us approximately evaluate the resulting envelope of the notched photoionization cross-section (53), assuming that the ‘longitudinal’ matrix elements ( $\dots$ ) constructions in equations 30–32 do not depend on  $K_{\perp}$ . The ‘transverse’ matrix elements can be evaluated following Potekhin & Pavlov (1997): in the perturbation approximation, they are proportional to  $|\xi|^{\delta m} e^{-|\xi|^2/2}$ , where  $|\xi|^2 = K_{\perp}^2 \rho_0^2 / (2\hbar^2)$ . Then,

$$\begin{aligned} \sigma(\omega < \omega_{\text{thr}}, K_{\perp}) &\approx \sigma(\omega_{\text{thr}}, 0) \exp \left[ -\frac{M_{\perp}}{M} \frac{\omega_{\text{thr}} - \omega}{\Omega_c} \right] \\ &\times \theta \left( \frac{K_{\perp}^2}{2M_{\perp}} - \hbar(\omega_{\text{thr}} - \omega) \right), \end{aligned} \quad (54)$$

where  $\theta(x)$  is the step function. A comparison of this approximation with numerical calculations for the hydrogen atom (Potekhin & Pavlov 1997) shows that it gives the correct qualitative behaviour of  $\sigma(\omega, K_{\perp})$ . For a quantitative agreement, one should multiply the exponential argument by a numerical factor  $\sim 0.5$ – $2$ , depending on the state and polarization. This numerical correction is likely due to the neglected  $K_{\perp}$ -dependence of the longitudinal matrix elements. We assume that this approximation can be also used for the helium atom. Using equation (52), we obtain

$$\sigma(\omega) \approx \sigma(\omega_{\text{thr}}) \exp \left[ -\frac{M_{\perp}}{M} \frac{\omega_{\text{thr}} - \omega}{\Omega_c} - \frac{\hbar(\omega_{\text{thr}} - \omega)}{k_B T} \right] \quad (55)$$

for  $\omega < \omega_{\text{thr}}$ . Here, the transverse mass  $M_{\perp}$  can be evaluated by treating the coupling Hamiltonian  $H_2$  as a perturbation, as was done by Pavlov & Mészáros (1993) for the H atom. Following this approach, retaining only the main perturbation terms according to the approximate orthogonality relation (33) and neglecting the difference between  $M$  and  $M_0$ , we obtain an estimate

$$\frac{M}{M_{\perp}} \approx 1 - \sum_{\alpha=\pm} \frac{\alpha}{2} \sum_{b(\Delta m=\alpha)} \frac{\omega_c f_{ba}^{\alpha} / (2\omega_{ba})}{1 + \omega_{ba} / \Omega_c}, \quad (56)$$

where  $|a\rangle$  is the considered bound state ( $|00, 10\rangle$  or  $|00, 20\rangle$  for the examples in Figs 2–7) and  $|b\rangle$  are the final bound states to which  $\alpha = \pm$  transitions  $|a\rangle \rightarrow |b\rangle$  are allowed. According to equation (34), the numerator in equation (56) is close to  $m + 1$  for  $\alpha = +$  and to  $m$  for  $\alpha = -$ .

For the transitions from the ground state with polarization  $\alpha = -$ , which are strictly forbidden in the infinite ion mass approximation, using the same approximations as above we obtain the estimate  $\sigma_{-}(\omega) \propto \sigma_{+}(\omega) \hbar \Omega_c k_B T / (k_B T + \hbar \Omega_c)^2$ .

Examples of the photoionization envelope approximation, as described in equation (55), are shown in Figs 2–7. In Figs 6 and 7 (for  $B = 10^{14}$  G), in addition to the magnetic broadening, we see a significant shift of the maximum, which originates from the last term in equation (49). Such shift is negligible in Figs 4 and 5 because of the relatively small  $\Omega_c$  value for  $B = 10^{12}$  G.

Finally, let us note that the Doppler and collisional broadening of spectral features in a strong magnetic field can be estimated, following Pavlov & Mészáros (1993), Pavlov & Potekhin (1995) and Rajagopal et al. (1997). The Doppler spectral broadening profile is

$$\phi_D(\omega) = \frac{1}{\sqrt{\pi} \Delta \omega_D} \exp \left[ -\frac{(\omega - \omega_0)^2}{\Delta \omega_D^2} \right], \quad (57)$$

with

$$\Delta \omega_D = \frac{\omega_0}{c} \sqrt{\frac{2T}{M}} \left[ \cos^2 \theta_B + \frac{M_{\perp}}{M} \sin^2 \theta_B \right]^{-1/2}, \quad (58)$$

where  $\theta_B$  is the angle between the wave vector and  $\mathbf{B}$ . The collisional broadening is given by

$$\phi_{\text{coll}}(\omega) = \frac{\Lambda_{\text{coll}}}{2\pi} \frac{1}{(\omega - \omega_0)^2 + (\Lambda_{\text{coll}}/2)^2}, \quad (59)$$

with

$$\begin{aligned} \hbar \Lambda_{\text{coll}} &= 4.8 n_e a_0 r_{\text{eff}}^2 \left( \frac{k_B T}{\text{Ryd}} \right)^{1/6} \\ &= 41.5 \frac{n_e}{10^{24} \text{ cm}^{-3}} T_6^{1/6} \left( \frac{r_{\text{eff}}}{a_0} \right)^2 \text{ eV}, \end{aligned} \quad (60)$$

where  $n_e$  is the electron number density and  $r_{\text{eff}}$  is an effective electron–atom interaction radius, which is about the quantum-mechanical size of the atom. The convolution of the Doppler, collisional and magnetic broadening profiles gives the total shape of the cross-section. For bound–free transitions, the Doppler and collisional factors can be neglected, but for the bound–bound transitions they give the correct blue wings of the spectral features (cf. Pavlov & Potekhin 1995).

## 6 CONCLUSION

We have presented detailed numerical results and fitting formulae for the dominant radiative transitions (both bound–bound and bound–free) of He atoms in strong magnetic fields in the range of  $10^{12}$ – $10^{14}$  G. These field strengths may be most appropriate for the identification of spectral lines observed in thermally emitting isolated NSs (see Section 1).

While most of our calculations are based on the infinite-nucleus-mass approximation, we have examined the effects of finite nucleus mass and atomic motion on the opacities. We found that for the field strengths considered in this paper ( $B \lesssim 10^{14}$  G), these effects can be incorporated into the infinite-mass results to obtain acceptable He opacities for NS atmosphere modelling. For large field strengths, more accurate calculations of the energy levels and radiative transitions of a moving He atom will be needed in order to obtain reliable opacities.

## ACKNOWLEDGMENTS

This work has been supported in part by NSF grant AST 0307252 and *Chandra* grant TM6-7004X (Smithsonian Astrophysical Observatory). The work of AYP is supported in part by FASI (Rosnauka) grant NSh-9879.2006.2 and RFBR grants 05-02-16245 and 05-02-22003.

## REFERENCES

- Abrahams A. M., Shapiro S. L., 1991, *ApJ*, 382, 233  
 Al-Hujaj O.-A., Schmelcher P., 2003a, *Phys. Rev. A*, 67, 023403  
 Al-Hujaj O.-A., Schmelcher P., 2003b, *Phys. Rev. A*, 68, 053403  
 Armstrong B. M., Nicholls R. W., 1972, *Emission, Absorption, and Transfer of Radiation in Heated Atmospheres*. Pergamon, Oxford  
 Baye D., Vincke M., 1990, *Phys. Rev. A*, 42, 391  
 Beloborodov A., Thompson C., 2007, *ApJ*, 657, 967  
 Bezchastnov V. G., Pavlov G. G., Ventura J., 1998, *Phys. Rev. A*, 58, 180  
 Burwitz V., Haberl F., Neuhäuser R., Predehl P., Trümper J., Zavlin V. E., 2003, *A&A*, 399, 1109  
 Chandrasekhar S., 1945, *ApJ*, 102, 223  
 Chang P., Arras P., Bildsten L., 2004, *ApJ*, 616, L147  
 Chen Z. H., Goldman S. P., 1992, *Phys. Rev. A*, 45, 1722  
 Cohen R., Lodenquai J., Ruderman, M., 1970, *Phys. Rev. Lett.*, 25, 467  
 De Luca A., Mereghetti S., Caraveo P. A., Moroni M., Mignani R. P., Bignami G. F., 2004, *A&A*, 418, 625  
 Haberl F., 2006, *Ap&SS*, 308, 181  
 Haberl F., Schwöpe A. D., Hambaryan V., Hasinger G., Motch C., 2003, *A&A*, 403, L19  
 Haberl F., Turolla R., de Vries C. P., Zane S., Vink J., Me'ndez M., Verbunt F., 2006, *A&A*, 451, L17  
 Harding A. L., Lai D., 2006, *Rept. Prog. Phys.*, 69, 2631  
 Ho W. C. G., Lai D., 2001, *MNRAS*, 327, 1081  
 Ho W. C. G., Lai D., 2003, *MNRAS*, 338, 233  
 Ho W. C. G., Lai D., 2004, *ApJ*, 607, 420  
 Ho W. C. G., Lai D., Potekhin A. Y., Chabrier G., 2003, *ApJ*, 599, 1293  
 Ho W. C. G., Kaplan D. L., Chang P., van Adelsberg M., Potekhin A. Y., 2007, *MNRAS*, 375, 821  
 Ivanov M. V., 1994, *J. Phys. B*, 27, 4513  
 Ivanov M. V., Schmelcher P., 2000, *Phys. Rev. A*, 61, 022505  
 Jones M. D., Ortiz G., Ceperley D. M., 1999, *Phys. Rev. A*, 59, 2875  
 Kaspi V. M., Roberts M., Harding A. K., 2006, in Lewin W., van der Klis M., eds, *Compact Stellar X-ray Sources*. Cambridge Univ. Press, Cambridge, p. 279  
 Lai D., 2001, *Rev. Mod. Phys.*, 73, 629  
 Lai D., Ho W. C. G., 2002, *ApJ*, 566, 373  
 Lai D., Ho W. C. G., 2003, *ApJ*, 588, 962  
 Lai D., Salpeter E. E., 1997, *ApJ*, 491, 270  
 Lai D., Salpeter E. E., Shapiro S. L., 1992, *Phys. Rev. A*, 45, 4832  
 Landau L. D., Lifshitz E. M., 1977, *Quantum Mechanics*. Pergamon, Oxford.  
 Medin Z., Lai D., 2006, *Phys. Rev. A*, 74, 062507  
 Medin Z., Lai D., 2007, *Adv. Space Res.*, 40, 1466  
 Miller M. C., Neuhauser D., 1991, *MNRAS*, 253, 107  
 Mori K., Hailey C. J., 2002, *ApJ*, 564, 914  
 Mori K., Ho W. C. G., 2007, *MNRAS*, 377, 905  
 Mori K., Chonko J. C., Hailey C. J., 2005, *ApJ*, 631, 1082  
 Müller E., 1984, *A&A*, 130, 415  
 Neuhauser D., Langanke K., Koonin S. E., 1986, *Phys. Rev. A*, 33, 2084  
 Neuhauser D., Koonin S. E., Langanke K., 1987, *Phys. Rev. A*, 36, 4163  
 Pavlov G. G., Bezchastnov V. G., 2005, *ApJ*, 635, L61  
 Pavlov G. G., Mészáros P., 1993, *ApJ*, 416, 752  
 Pavlov G. G., Potekhin A. Y., 1995, *ApJ*, 450, 883  
 Potekhin A. Y., 1994, *J. Phys. B*, 27, 1073  
 Potekhin A. Y., Chabrier G., 2003, *ApJ*, 585, 955  
 Potekhin A. Y., Chabrier G., 2004, *ApJ*, 600, 317  
 Potekhin A. Y., Pavlov G. G., 1993, *ApJ*, 407, 330  
 Potekhin A. Y., Pavlov G. G., 1997, *ApJ*, 483, 414  
 Potekhin A. Y., Pavlov G. G., Ventura J., 1997, *A&A*, 317, 618  
 Potekhin A. Y., Chabrier G., Shibano Yu. A., 1999, *Phys. Rev. E*, 60, 2193 (Erratum: *Phys. Rev. E*, 63, 01990)  
 Potekhin A. Y., Lai D., Chabrier G., Ho W. C. G., 2004, *ApJ*, 612, 1034  
 Potekhin A. Y., Chabrier G., Lai D., Ho W. C. G., van Adelsberg M., 2006, *J. Phys. A: Math. Gen.*, 39, 4453  
 Pröschel P., Rösner W., Wunner G., Ruder H., Herold H., 1982, *J. Phys. B*, 15, 1959  
 Rajagopal M., Romani R., Miller M. C., 1997, *ApJ*, 479, 347  
 Relovsky B. M., Ruder H., 1996, *Phys. Rev. A*, 53, 4068  
 Sanwal D., Pavlov G. G., Zavlin V. E., Teter M. A., 2002, *ApJ*, 574, L61  
 Schmelcher P., Cederbaum L. S., 1991, *Phys. Rev. A*, 43, 287  
 Schmelcher P., Ivanov M. V., Becken W., 1999, *Phys. Rev. A*, 59, 3424  
 Scrinzi A., 1998, *Phys. Rev. A*, 58, 3879  
 Shibano Yu. A., Pavlov G. G., Zavlin V. E., Ventura J., 1992, *A&A*, 266, 313  
 Sokolov A. A., Ternov I. M., 1986, *Radiation from Relativistic Electrons*, 2nd rev. edn. AIP, New York  
 Thurner G., Körbel H., Braun M., Herold H., Ruder H., Wunner G., 1993, *J. Phys. B*, 26, 4719  
 Turbina A. V., Guevara N. L., 2006, *Phys. Rev. A*, 74, 063419  
 van Adelsberg M., Lai D., 2006, *MNRAS*, 373, 1495  
 van Adelsberg M., Lai D., Potekhin A. Y., Arras P., 2005, *ApJ*, 628, 902  
 van Kerkwijk M. H., Kaplan D. L., 2007, *Ap&SS*, 308, 191  
 van Kerkwijk M. H., Kaplan D. L., Durant M., Kulkarni S. R., Paerels F., 2004, *ApJ*, 608, 432  
 Vincke M., Baye D., 1988, *J. Phys. B*, 21, 2407  
 Vincke M., Baye D., 1989, *J. Phys. B*, 22, 2089  
 Zane S., Turolla R., Stella L., Treves A., 2001, *ApJ*, 560, 384  
 Zane S., Cropper M., Turolla R., Zampieri L., Chierigato M., Drake J. J., Treves A., 2005, *ApJ*, 627, 397

This paper has been typeset from a  $\text{\TeX}/\text{\LaTeX}$  file prepared by the author.